An extremely fast neural mechanism to detect emotional visual stimuli: A two-experiment study

Carretié, Luis*[,1]; Fernández-Folgueiras, Uxía [1]; Kessel, Dominique [1] ; Alba, Guzmán[1]; Veiga-Zarza, Estrella[1]; Tapia, Manuel[1]; Álvarez, Fátima [1];

[1] *Facultad de Psicología, Universidad Autónoma de Madrid, 28049 Madrid, Spain*

* Corresponding author: Luis Carretié, Facultad de Psicología, Universidad Autónoma de Madrid, 28049 Madrid, Spain. E-mail: carretie@uam.es

Short title: Fast detection of emotional visual stimuli

ABSTRACT

Defining the brain mechanisms underlying initial emotional evaluation is a key but unexplored clue to understand affective processing. Event-related potentials (ERPs), especially suited for investigating this issue, were recorded in two experiments (n=36 and n=35). We presented emotionally negative (spiders) and neutral (wheels) silhouettes homogenized regarding their visual parameters. In Experiment 1, stimuli appeared at fixation or in the periphery (200 trials per condition and location), the former eliciting a N40 (39 milliseconds) and a P80 (or C1: 80 milliseconds) component, and the latter only a P80. In Experiment 2, stimuli were presented only at fixation (500 trials per condition). Again, a N40 (45 milliseconds) was observed, followed by a P100 (or P1: 105 milliseconds). Analyses revealed significantly greater N40-C1P1 peak-to-peak amplitudes for spiders in both experiments, and ANCOVAs showed that these effects were not explained by C1P1 alone, but that processes underlying N40 significantly contributed. Source analyses pointed to V1 as a N40 focus (more clearly in Experiment 2). Sources for C1P1 included V1 (P80) and V2/LOC (P80 and P100). These results and their timing point to low-order structures (such as visual thalamic nuclei or superior colliculi) or the visual cortex itself, as candidates for initial evaluation structures.

KEYWORDS

Emotion, initial evaluation, ERPs, N40, P80, P100, visual cortex.

INTRODUCTION

Despite the growing interest and knowledge on the neural mechanisms sustaining emotional processing, several basic, key issues remain far from being understood. One of them, especially relevant in evolutionary terms, is how the brain deals so rapidly with emotional stimulation, organizing behavioral reactions that, in some circumstances, occur within four of five-tenths of a second (e.g., Zhang & Lu, 2012). An obvious and necessary previous neural process is detecting emotional stimuli or, in other words, initially evaluate the incoming sensory input and mark it, if pertinent, as dangerous, appetitive, or, in general, affectively loaded. These initial evaluation structures (IESs) are still undefined, despite several hypotheses have been proposed. An intimately related and unsolved issue is the latency at which these structures can elicit electrophysiological traces, by themselves or through their cortical projections, of their evaluative activity. Crucially, this latency may help to reinforce some of the proposals on IESs over others.

For example, the detection of subliminal facial expressions by the amygdala, often conceptualized as a core IES (e.g., see reviews or meta-analyses in Adolphs, 2008; Costafreda et al., 2008; Öhman, 2002; Zald, 2003), lasts more than 250 milliseconds (ms) to be reflected in the visual cortex (Wang et al., 2023). However, the visual cortex shows greater activity to emotional stimuli than to neutral ones before 100 ms (Carretié et al., 2022). Thus, it is improbable that this early visual cortical activity is mediated by the amygdala. Moreover, while emotional faces elicit an increased response in the amygdala as compared to neutral faces as soon as 74 ms, amygdalar discrimination of emotional *non-facial* stimuli occurs beyond 150 ms from stimulus onset (Méndez-Bértolo et al., 2016). Again, evidence exists of visual cortex discrimination of emotional non-facial stimuli before 100 ms (Carretié et al., 2022). In other words, current data point to candidates other than the amygdala to be IESs. An alternative hypothesis is that initial -albeit rudimentary- evaluation may reside in faster (≈30-ms) first-order structures (i.e., receiving direct visual inputs from the retina). This low-order IES

hypothesis (Carretié et al., 2021) points to the visual thalamus, mainly the lateral geniculate nucleus (LGN)-thalamic reticular nucleus (TRN) tandem, which are recently being revealed as active processors of the visual input rather than passive relays, as traditionally assumed (see reviews in Fiebelkorn & Kastner, 2020; Ghodrati et al., 2017), with the contribution of other first- and second-order thalamic and non-thalamic nuclei such as the superior colliculus (e.g., Méndez et al., 2022). Finally, a third hypothesis is that the visual cortex itself is the initial evaluator, its activity being not relevantly mediated by any previous evaluation process (Li & Keil, 2023).

Thus, the latency of the first biased response to emotional stimuli in the visual cortex indirectly informs on the nature of the IES involved. Particularly, shorter latencies would support non-amygdalar hypotheses. The best non-invasive methodologies to study response latencies of human neural processes are magnetoelectric (EEG and MEG), whose temporal resolution is much higher than that of the rest of non-invasive neuroimaging techniques. In the visual domain, the earliest trace in event-related potentials (ERPs) -one of the neural signals the EEG provides- signaling cortical processing is usually attributed to the C1 component. This component initiates at ≈60 ms from stimulus onset and peaks at ≈80, and is mainly originated in the striate cortex or V1 (Capilla et al., 2016; Di Russo et al., 2003), although the contribution of V2 and V3 has also been raised (Ales et al., 2010; Capilla et al., 2016). Importantly, C1 peak shows enhanced amplitudes in response to emotional facial expressions as compared to neutral at around 80 ms (Acunzo et al., 2019; Eldar et al., 2010; Pourtois et al., 2004). Non-facial, consciously perceived emotional stimuli have not been explored in this respect.

Although less frequently, visual ERP components before C1 have also been reported (Buchner et al., 1997; Ffychte et al., 1995; Foxe & Simpson, 2002; Inui & Kakigi, 2006; Moradi et al., 2003; Proverbio et al., 2002; Yoshida et al., 2017). This pre-C1 activity, which lacks a consensual nomenclature, will be referred to as N40 hereafter. The scarce data available on

the origin of N40 point to V1 as one of its sources. Indeed, the onset of V1 activity once the geniculo-cortical inputs arrive may occur as early as 18-20 ms in the macaque monkey (Maunsell & Gibson, 1992; Schroeder et al., 1998) with an average latency reported at 26 ms (Schroeder et al., 1998). An extrapolation to humans following the rough 3/5 ratio characterizing macaque vs human latencies (e.g., Kelly et al., 2013) yields an approximate latency of 40 ms in our species. The contribution of V1 to the generation of N40 has also been reported in humans (Proverbio et al., 2010) along with thalamic sources (Proverbio et al., 2021). Interestingly, N40 has been revealed to be modulated by attention, so it appears to be sensitive to cognitive factors (Proverbio et al., 2002; 2021). Modulation of such an early ERP activity by emotional stimuli has not been explored yet, however. Thus, the scarce studies exploring these extremely early electrophysiological traces of visual processing employ non-emotional stimuli. On the other hand, ERP studies presenting emotional stimuli have not been designed to explore N40, which presents a relatively low amplitude and hence, low signal-to-noise ratio (SNR).

We carried out two experiments to explore whether ERP activity originating in the visual cortex during the first 100 ms is enhanced by non-facial, supraliminal, emotional visual stimuli in order to advance in the characterization of IESs. To this aim, we introduced several methodological implementations that help to enhance the SNR in early visual ERP components. First, the number of trials was larger than usual in ERP research on emotional stimulation. Second, stimuli presented Gestalt characteristics such as closed contours or compact shape (they consisted of silhouettes) since they are optimal to increase the response of contour-sensitive neurons present in V1 and V2 (e.g., Ko & von der Heydt, 2018). Third, in Experiment 1, stimuli were presented at several spatial locations given that cognitive (attentional) and emotional effects on early visual ERP components (such as C1) may be modulated (and even neutralized) depending on their position in the visual field (attentional effects: Mohr & Kelly 2018; emotional: Carretié et al., 2022). Experiment 2 employed only

stimuli at fixation given the results of Experiment 1, and this allowed for a further increase in the number of trials. This second experiment also included several design modifications to control for potential alternative explanations of the effects observed in Experiment 1.

EXPERIMENT 1

Materials and Methods

Participants

Forty-four individuals participated in this experiment, although data from only 36 of them could eventually be analyzed (this sample allows reaching a statistical power of at least 0.8 for two dependent means comparisons -spiders vs. wheels, in this case- foreseeing medium effect sizes, usual in studies on early ERPs; computations were carried out employing G*Power© developed by Faul et al., 2009). These 36 participants (age range of 18 to 24 years, mean=19.46, SD=1.14, 29 women) were students of Psychology, provided their written informed consent, and received academic compensation for their participation. The study was designed in accordance with the Declaration of Helsinki and had been previously approved by the Universidad Autónoma de Madrid's Ethics Committee. The whole sample of participants attended the laboratory between November 10 and 30, 2020.

Stimuli and procedure

Participants were placed in an electrically shielded, sound-attenuated room. They were asked to place their chin on a chinrest maintained at a fixed distance (40 cm) from the screen (VIEWpixx®, 120 Hz) throughout the experiment. Two types of stimuli were presented to participants (Figure 1): 20 emotional silhouettes (spiders) and 20 neutral (wheels), all in black color over a white background. Spiders are among the top five most feared animals (Gerdes et al., 2009), and they cause the most prevalent phobia related to animals (Jacobi et al., 2004). Indeed, spiders are assessed as negatively valenced stimuli by relatively large samples in emotional picture databases (e.g., IAPS: Lang et al., 2005; EmoMadrid: Carretié et al., 2019). In

order to test whether spider *silhouettes* were also efficient as negatively valenced stimuli, and wheels as neutral, they were previously evaluated by an independent sample of 447 participants (397 women, mean age=19.51, SD=1.46) who rated their emotional valence through a 7-point Likert scale that ranged from "very negative" (1) to "very positive" (7). Spiders were rated as negative (mean=1.704, standard error of means [SEM]=0.038) and wheels as neutral (i.e., in the intermediate values of the scale: mean=3.918, SEM=0.030). Differences between both stimuli were strongly significant ($F(1,446)=2557.289$, $p<0.001$, $\eta^2_p=0.852$).

*** Figure 1 ***

As mentioned in the introduction, stimuli presenting Gestalt characteristics such as closed contours or compact shape, as it is the case of silhouettes, are optimal to increase the response of contour-sensitive neurons present in V1 and V2 (Ko & von der Heydt 2018). Moreover, the use of black silhouettes over white background inherently equalizes color and contrast, which may influence early visual ERPs (color: Paulus et al. 1984; contrast: Foxe et al. 2008), across experimental categories. Luminosity (i.e., figure surface against background) and spatial frequency of silhouettes, which may also influence ERP components of interest (luminosity: Johannes et al. 1995; spatial frequency: Nakashima et al. 2008), were manipulated so they did not significantly differ between categories (spiders vs. wheels). Details on these two low-level characteristics and statistical contrasts, as well as stimuli themselves, are provided in EmoMadrid (https://www.psicologiauam.es/CEACO/EmoMadrid/EMsiluetas.htm). In sum, the only visual parameter besides their emotional meaning clearly differing among spiders and wheels was their shape, in any case sharing certain key characteristics (e.g., wheel spokes may resemble spider legs and vice versa). More importantly, shape per se has been reported to firstly affect ERPs in latencies longer than those explored in this study (Bradley et al. 2007; Hillyard et al. 1998; Van Strien et al, 2016).

The size of stimuli (figure + ground) was 14º x 14º width. Each spider and wheel appeared 10 times in random order in one of the five locations depicted in Figure 1, one at fixation (FIX) and four peripheral (the center of each peripheral position was 32.5º from the center of the screen). Peripheral positions were upper-left visual field (UL), upper-right (UR), lower-left (LL) and lower-right (LR). This resulted in 200 trials per emotional category and location (20 exemplars x 10 presentations), and the total number of trials was 2000 (200 x 2 categories x 5 locations). Each stimulus, whatever its location, was displayed on the screen for 150 ms, and interstimulus interval was 850 ms. Participants were instructed to look at the fixation dot at the center of the screen all the time, which was marked with a blue circle (0.3 º radius, RGB=0, 0, 255) during the interstimulus intervals. The total duration of the whole stimulus sequence was ≈32 minutes, so it was divided into eight blocks to provide brief rest periods. In order to engage constant attention to stimulation, the inter-stimulus fixation dot randomly changed its color from blue to red (255, 0, 0) in 1 to 5 trials per block (0.5-2.5% trials per block), and participants were instructed to mentally count these changes and report the total number after each block (this sum was different from block to block). None of the participants deviated more than one color change from the correct answer per block. As explained later, each red dot trial, and the next, were removed prior to analyses.

Recording and pre-processing

Electroencephalographic (EEG) activity was recorded using an electrode active cap (Biosemi®) with Ag-AgCl electrodes, in which the EEG signal is preamplified at the electrode. Sixty-four electrodes were placed at the scalp attending a homogeneous distribution and the international 10-20 system. Following the BioSemi design, the voltage at each active electrode was recorded with respect to a common mode sense (CMS) active electrode and a passive electrode (DRL) replacing the ground electrode. All scalp electrodes were referenced offline to the nosetip. Electrooculographic (EOG) data were recorded supra- and infraorbitally (vertical

EOG) as well as from the left versus right orbital rim (horizontal EOG) to detect blinking and ocular deviations from the fixation point. An online analog low-pass filter was set to 104Hz (5th order, CIC filter), with no high-pass filter. Recordings were continuously digitized at a sampling rate of 512 Hz. An offline digital Butterworth bandpass filter of 0.01 to 30 Hz (2nd order, zero-phase forward and reverse –twopass- filter) was applied to continuous (pre-epoched) data using the Fieldtrip software (http://fieldtrip.fcdonders.nl; Oostenveld et al., 2011). Setting the high-pass filter at 0.1 Hz or less has been recommended to study early ERP components (Acunzo et al., 2012). The continuous recording was divided into 300 ms epochs per trial, beginning 100 ms before the probe stimulus onset. The inevitable lag between the marks signaling stimuli onsets (or 'triggers') in EEG recordings and its actual onset on the screen was measured employing a photoelectric sensor as described in https://www.youtube.com/watch?v=0BPwcciq8u8 and corrected during pre-processing.

EEG epochs corresponding to trials in which the fixation dot changed its color (see the previous section) were eliminated, as well as those corresponding to the subsequent trial, to avoid the effect of this control, irrelevant (to our scopes) task. Blinking-derived artifacts were removed through an independent component analysis (ICA)-based strategy (Jung et al., 2000), as provided in Fieldtrip. After the ICA-based removal process, a second stage of inspection of the EEG data was conducted to automatically discard trials in which any EEG channel surpassed ±100 µV and/or its average global amplitude (i.e., maximum minus minimum amplitude) across trials ± 3.5 standard deviations. The minimum number of trials accepted for averaging was 150 trials per participant and condition (i.e., each category presented in each location). Data from six of the discarded participants (see Participants section) were eliminated since they did not meet this criterion, and the other two had to be discarded because of data storage issues. This trial and participant rejection procedure led to the average admission of 179 (*SD=7*), 180 (*8*), 181 (*8*), 182 (*8*), and 181 (*7*) trials at each of the five locations in the case of spiders, and of 181 (*SD=8*), 181 (*7*), 180 (*8*), 181 (*7*), and 180 (*9*) in the case of wheels, the

difference among stimulus categories being non-significant ($F(9,315)=0.915$, $p=0.512$, $\eta^2_p=0.025$).

Data and supplemental material availability

The data associated with this experiment are available at https://osf.io/9bc2y. Supplemental material mentioned hereafter is also available at that link.

Data analysis

After baseline correction, the first analytic task was identifying and quantifying the first visual component of ERPs. As may be appreciated in Figure 2, a N40 component is visible in grand averages in response to FIX stimuli, being less evident in response to peripheral stimuli. To objectively confirm the existence or not of the N40 component, we determined whether amplitudes greater than typical baseline amplitude existed in its corresponding time window considering, at the same time, that N40 typically presents a very low SNR so too stringent criteria could mask this component. Thus, for each condition and within the 30-60 ms interval, the occurrence of N40 was confirmed when at least two neighbor channels (within the relevant scalp region, i.e., the posterior hemiscalp) presented at least two consecutive voltage points whose amplitude was beyond ±1.5 times the standard deviation of the corresponding baseline. This procedure revealed that N40 took place in the FIX conditions (both spiders and wheels), but not in any of the remaining eight conditions (four peripheral locations x two types of stimuli). To define N40 peak latency in response to FIX stimuli, recordings at parietal and occipital electrodes, bilaterally, were averaged together to provide a meta-average (Figure 2). The latency of the most negative value of the meta-average between 30 and 60 ms was defined as the N40 peak, which was 39 ms. Therefore, N40 amplitude to FIX stimuli was individually quantified as the average amplitude within the 36 to 42 ms window of interest (WOI).

*** Figure 2 ***

The next component in time (P80) was also detected and its amplitude quantified in all conditions, since it was patent in all of them, including peripheral (Figure 2). Thus, P80 peak latency was defined by averaging together recordings at parietal and occipital electrodes, bilaterally in the case of FIX stimuli and contralaterally for peripheral stimuli, to obtain meta-averages (Figure 2). The latency of the most positive value of meta-averages between 60 and 110 ms was defined as the P80 peak: 80 ms for FIX stimuli (WOI to compute individual amplitude: 74-86 ms), 88 for LL (WOI: 82-94 ms), 86 for LR (WOI: 80-92 ms), 90 for UL (WOI: 84-96), and 101 for UR (WOI: 95-107 ms): Table 1.

We also measured the differential N40-P80 amplitude, or peak to peak amplitude, a classical way of computing amplitudes (e.g., Begleiter et al., 1980; Hillyard & Picton, 1978; Verleger & Cohen, 1978) that has recently been revealed as useful to explore early visual ERP components (Carretié et al., 2022). Two advantages of this measure may be underlined. First, it is less susceptible to be affected by data processing settings such as the high-pass filter cut frequency, which significantly affects traditional (monophasic) amplitude measures in early components (Acunzo et al., 2012; Widmann & Schröger, 2012), or the length of the baseline, another critical aspect in this regard. Second, it allows to quantify neural processes transversally affecting neighbor components by eliciting an increase of absolute amplitude in both of them, as is apparently the case here (Figure 2). To this aim, the individual difference between P80 and N40 amplitudes (each computed as explained above) was calculated for FIX stimuli, given that peripheral stimuli did not elicit the N40 component (Figure 2).

To avoid the multiple comparison problem that analyses are potentially affected by, the experimental effects on N40 and P80 were analyzed by submitting their amplitudes in the corresponding WOIs to a spatial principal component analysis (sPCA) on SPSS 26.0 (IBM Corp., 2019). This procedure reduces the electrode information (64 levels) into a small number of

spatial factors (SFs) explaining, for the whole experimental sample, most of the variance due to the scalp location of recordings. The spatial factor score, the sPCA-derived single parameter (per participant and condition) in which each SF is quantified, "summarizes" the behavior of the whole set of electrodes it involves (with different weights) and is linearly related to original amplitudes. A separate sPCA was applied to each stimulus spatial location (FIX, LL, LR, UL, UR) given i) that N40 was only elicited by FIX stimuli and ii) that the latency of P80 varied across locations, as indicated. Components were selected based on the scree test and subsequently submitted to varimax rotation, which provides optimal performance in sPCA (Dien, 2010). Factor scores corresponding to those SFs showing a parietal/occipital distribution (bilateral for FIX conditions or contralateral to stimulus location for peripheral conditions), the one relevant as regards early visual ERPs, were then submitted to statistical contrasts. A double contrast strategy was carried out using JASP software (JASP Team, 2021). First, a one-tailed (given that our scope was detecting the earliest trace of sensory gain -i.e., greater activity in visual processing structures- towards emotional stimuli) frequentist repeated-measures Student's T-test was carried out introducing Emotion of the probe (spiders, wheels) as factor. Effect sizes in these tests were computed using the Cohen's d formula. Second, Bayesian paired samples T-tests using the default prior (0.707), corresponding to medium effect sizes as indicated above, were carried out on the same data to test the likelihood of data on H1 (spider > wheel) over H0 (spider = wheel) (BF10).

Finally, and to better characterize N40 and P80, their sources were estimated via the Minimum Norm (MN) method using the current density map algorithm as implemented in Brainstorm (Tadel et al., 2011; v2021). To this aim, average amplitudes within the WOIs of each component showing significant effects in the previous (statistical contrast) step were submitted to this algorithm (depth weighting order and maximal amount: 0.5 and 10, respectively; noise covariance regularization: 0.1; SNR: 10), which was applied on a realistic cortex model defined through the openMEEG package (Gramfort et al., 2010; Kybic et al.,

2005). However, source estimations of the P80 component recorded in conditions showing insensitivity to the experimental treatment (i.e., peripheral conditions) are also available at Supplemental material.

Results

N40 (stimuli at fixation)

The sPCA was computed on N40 amplitudes to FIX stimuli only, as explained above. This analysis yielded five SFs as explaining most of the variance of the 64 electrodes (88.11%). SF2 was the one showing bilateral occipital/parietal distribution which, for obvious reasons, is the one relevant in this case. Figures 2 and 3 show the topography of N40-SF2, and Figure 3 depicts meta-averaged recordings from representative electrodes of this SF, along with descriptive plots. Its corresponding factor scores were then submitted to repeated-measures T-tests, both frequentist and Bayesian, on factor Emotion (spiders, wheels). As shown in Table 1, the former yielded significant differences (t(35)= -1.747, p=0.045, d=-0.291), spiders showing more negative N40 scores/amplitudes (Figure 3). However, Bayesian analyses found only anecdotal evidence in favor of H1 (greater N40 amplitude -more negative- for spiders than for wheels): BF_{10}=1.342.

*** Figure 3 ***

		Peak	WOI	SFs (% var)	T(35)	p	Cohen d's	BF_{10} (Bayes)
N40	**FIX**	39	36-42	5 (92.7)	**-1.747**	**0.045**	**-0.291**	1.342
P80	**FIX**	80	74-86	5 (92.7)	**3.525**	**<0.001**	**0.588**	**53.470**
	LL	88	82-94	4 (87.5)	-0.589	0.720	-0.098	0.121
	LR	86	80-92	5 (88.8)	-1.582	0.094	-0.264	0.075
	UL	90	84-96	4 (86.6)	-2.134	0.980	-0.356	0.062
	UR	101	95-107	6 (88.9)	-0.743	0.769	-0.124	0.110
N40-P80	**FIX**	-	-	5 (93.5)	**4.547**	**<0.001**	**0.758**	**764.941**

Table 1. Experiment 1: peak latencies (in milliseconds), windows of interest (WOIs), number of spatial factors (SFs) extracted in sPCA, total variance they explain (% var), and outputs of both Student's frequentist and Bayesian t-tests on the spider>wheel difference corresponding to N40 and P80 amplitudes (FIX: fixation, LL: lower left, LR: lower right, UL: upper left, UR: upper right).

MN source estimation analysis on N40 elicited by FIX stimuli was carried out on the average amplitude within the N40 WOI, as indicated. As illustrated in Figure 2, this analysis yielded V1 as one of the sources (concretely, the caudal apex of the calcarine sulcus), but also other foci at prefrontal areas (Table 2). This disparity of sources may point to a low SNR and to possible spurious solutions rather than to a spread cortical activation, an issue that will be discussed later and that was addressed in Experiment 2.

N40		P80	
x, y, z	**Anatomical label**	**x, y, z**	**Anatomical label**
20, -100, 0	Calcarine sulcus	-11, -105, -12	Calcarine sulcus
4, 73, 1	SFG, frontal pole	30, -101, 2	Middle occipital gyrus
-55, 43, 7	IFG, pars triangularis		

Table 2. Experiment 1: main sources estimated through the Minimum Norm method for N40 and P80 in response to FIX stimuli (both spiders and wheels) and their peak MNI coordinates.

P80 (stimuli at fixation and at the periphery)

P80 was clearly elicited by all stimuli, whatever their location, so sPCAs were applied to all conditions. Table 1 shows the number of SFs extracted for each stimulus spatial location in the case of P80, and their total explained variance, which was over 86% in all cases. Factorial loadings corresponding to those SFs showing occipital/parietal distribution, bilateral in the case of FIX stimuli and contralateral in the case of peripheral stimuli, which were those relevant to our scopes (i.e., SF5 for FIX, SF4 for UL, SF2 for UR and LL, and SF3 for LR), are represented in Figures 2 and 3.

Factor scores derived from each SF were subsequently contrasted via repeated-measures T-tests on factor Emotion (spiders, wheels) and, since five contrasts were carried out (one per stimulus location), alpha was submitted to the Bonferroni adjustment procedure to avoid multiple comparison-derived type I errors. This adjustment set alpha at 0.01. Spiders

elicited significantly greater P80 amplitudes than wheels when they were presented at fixation ($t(35)= 3.525$, $p<0.001$, $d=0.588$): Figure 3. Instead, peripheral conditions did not yield significant spiders>wheels differences: Table 1. On the other hand, Bayesian analyses confirmed strong evidence in favor of H1 (spiders>wheels) in the case of FIX stimuli: $BF_{10}=53.470$, and null evidence (or even strong evidence in favor of H0) for peripheral conditions (Table 2). However, peripheral stimuli were actually perceived and discriminated, as revealed by later ERP components (these analyses and their results are described in Supplemental material for being out of the scope of this study).

Source estimation on P80 amplitude to FIX stimuli returned V1, bilaterally, as the main focus of activity (x=-11, y=-105, z=-12; Figure 2), along with bilateral foci in V2/LOC -lateral occipital cortex- (x=-30, y=-101, z=2) with no other relevant foci in the rest of the cortex (V3, also present in this area, is an unlikely source since its main role is color processing). Supplemental material also includes source estimation of P80 to peripheral conditions, showing how main foci were located at visual cortices contralateral to stimulus location, more dorsally when presented in the lower visual field, and more ventrally for stimuli in the upper visual field.

<u>N40-P80 peak-to-peak amplitudes (stimuli at fixation)</u>

Finally, N40-P80 differential amplitude was computed as the difference of the amplitudes of both components, each measured as indicated above, in response to FIX stimuli. These differences, calculated for each channel, condition (spider or wheel) and participant, were then submitted to a sPCA. The critical factor in this case was SF5 which, as illustrated in Figures 2 and 3, presented maximal loadings at midline parietal/occipital areas. The repeated-measures T-test contrasting its factor scores as a function of factor Emotion (spiders, wheels) yielded significantly greater N40-P80 peak to peak amplitude to spiders than to wheels, this result showing a large effect size ($t(35)= 4.547$, $p<0.001$, $d=0.758$). The Bayesian repeated-

measures T-test on these data found 'extreme' evidence in favor of H1 (spiders>wheels): BF10=764.941.

In order to test whether this significant sensitivity of N40-P80 peak-to-peak factor scores or amplitudes could be explained by either N40 or P80 alone (being in this case a redundant result), a repeated-measures ANCOVA was carried out using SPSS 26.0. In it, N40-P80 peak-to-peak amplitudes were introduced as dependent variable, and N40 and P80 amplitudes, separately, as covariates. The covariates were both significantly related to the N40-P80 peak-to-peak amplitude [N40: $F(1, 54.931)=10.144$, $p=0.002$); P80($1, 62.322)=133.905$, $p<0.001$). Indeed, the effect of Emotion of the probe on N40-P80 peak to peak amplitude is lost after controlling for both N40 and P80 amplitudes [$F(1, 41.437)=3.598$, $p=0.065$]. In other words, N40-P80 peak-to-peak effects depend on both N40 and P80 and reflects a neural process transversally affecting both deflections.

Discussion

Our results confirm the capability of our visual system to rapidly detect certain emotional stimuli but reveal that this may begin earlier than previously found, beginning at 39 ms (36-42 ms window) from stimulus onset. This is partially revealed by N40, which shows mixed evidence in frequentist and Bayesian contrasts and, robustly, by the N40-P80 peak-to-peak amplitude. This extremely fast activity reflecting the discrimination of emotional visual stimuli, and manifested in N40-P80, was statistically demonstrated to be due to both N40 and P80, and not to any of them separately. The visual cortex was found to be in the origin of both components. In the case of N40, solutions included V1. This first visual cortex stage receives the majority of inputs from the lateral geniculate nucleus of the thalamus (Hubel & Wiesel, 1972). Additionally, source estimation solutions unexpectedly included prefrontal areas, whose involvement seems improbable at this latency. These prefrontal foci likely reveal analytical noise and point to the desirability of increasing SNR in the second experiment. P80 sources were cleaner and also involved V1, along with V2 and/or lateral occipital cortex (LOC). Both V2

and LOC are involved in object recognition in a progressive way, from contour and shape processing in V2 (Anzai et al., 2007) to more global object identification in LOC (Grill-Spector et al., 2001).

The theoretical implications of this extremely fast discrimination in early visual cortices, carried out during the whole 40-80 ms window from stimulus onset, will be considered in the General Discussion section. However, it is important to underline here the novelty of these results as Experiment 1 is the first, to the best of our knowledge, to report the discrimination of emotional visual stimuli so early in time. This is understandable since pre-C1 activity, already little studied, has not been explored in response to emotional stimuli, either because studies analyzing this early visual ERP activity employed neutral stimuli or because experiments presenting emotional stimuli were not oriented nor designed to record this activity. In any case, we designed and carried out a second experiment in order to replicate these findings. First, further increasing the number of trials was considered a priority in Experiment 2 in order to boost SNR for the reasons explained above. In addition, to increase this ratio, a jitter was added to the inter-trial interval to avoid a phase-locking of alpha EEG activity with the stimulus presentation rate. Third, we changed the color of the fixation dot. In Experiment 1, the contrast between the fixation dot (dark blue) and either the figure (black) or the background (white) was unbalanced between spiders and wheels when they were presented at fixation: the dot was surrounded by the figure -black- in 85% (i.e., less contrast) of the spider trials and in 25% of the wheel trials. Thus, we presented exactly the same stimuli in the replication but used a grey (equidistant from white and black) fixation dot in order to discard any influence of this dot-stimulus contrast in the observed effects.

And fourth, Experiment 2 presented stimuli only at fixation. Indeed, stimuli at the periphery (i.e, projected to the perifoveal region in our study) failed to elicit the N40 component or to show significant differences between spiders and wheels in P80. However,

spider > wheel differences emerged in later, out of our scopes, ERP components, as shown in Supplemental material, demonstrating that these stimuli were actually perceived and evaluated. Two methodological factors may contribute to explain the unexpected lack of sensitivity to peripheral stimuli of the earliest ERP components. First, SNR in early visual components is even lower for peripheral vision since it is underrepresented (compared to foveal vision), in terms of number of neurons involved, both in the visual thalamus and in V1 (e.g., Azzopardi & Cowey, 1996). Second, the task asked to direct attention towards fixation (i.e., color changes in the fixation dot). Considering that attention yields a biased competition at the perceptual level whereby limited processing resources prioritize attended spatial locations over unattended ones (Beck and Kastner, 2005; Desimone, 1998), peripheral stimuli may have evoked diminished activity for this reason as well. These issues are beyond the scopes of the second experiment -focused on stimuli at fixation- to avoid an excessive number of trials, but deserve to be explored in the future.

EXPERIMENT 2

The main scope of Experiment 2 was to replicate the novel findings revealing the capability of the visual cortex to discriminate emotional from non-emotional stimuli at extremely short latencies. This replication employed exactly the same stimulus exemplars, sizes, stimulus durations, average intertrial interval, and task. However, as indicated in the previous discussion, i) number of trials increased, ii) a jitter was added to the inter-trial interval, iii) fixation dot color was a grey tone equidistant from black and white, iv) stimuli were only presented at fixation. The details of these changes in the experimental design are described below.

Materials and Methods

Participants

Thirty-nine individuals, none of whom participated in Experiment 1, took part in Experiment 2. The data from only 35 of them (age range of 17 to 24 years, mean=19.68, SD=2.11, 30 women) could eventually be analyzed, as explained later. This sample size allows reaching a statistical power of at least 0.8 for two dependent means comparisons (spiders vs. wheels, in this case) foreseeing medium effect sizes, usual in studies on early ERPs (computations were carried out employing G*Power© developed by Faul et al., 2009). The study was designed in accordance with the Declaration of Helsinki and had been previously approved by the Universidad Autónoma de Madrid's Ethics Committee. All participants were students of Psychology, provided their written informed consent (that of the only participant under the legal age of majority in Spain -18 years- was also signed by one of her parents), and received academic compensation for their participation. The whole sample of participants attended the laboratory between September 18 and November 20, 2023.

Stimuli and procedure

The stimuli were identical to those employed in Experiment 1, and maintained the same size and duration. However, stimuli were presented only at fixation. Each category (spiders and wheels) was presented 500 times (vs. 200 in Experiment 1). In this second experiment, ITI presented five different durations (750, 800, 850, 900, 850 ms), the average being 850 ms (as Experiment's 1 fixed ITI). Finally, the fixation dot was grey (RGB: 128, 128, 128) during stimulus presentation and black (0, 0, 0) in the intertrial interval (since the background during ITI was also grey). The grey dot color was equidistant from black -figure- and white (255, 255, 255) -background- in terms of luminosity. As in Experiment 1, the presentation order was random and the total run (≈ 16 minutes) was divided into four blocks. In each of them, the black fixation dot changed to red instead of grey in 1 to 5 trials per block (0.5-2.5% trials per block)

and, as in Experiment 1, the task consisted in "mentally counting" the number of changes to red. Participants were asked to report the number of changes at the end of each block. The data from one of the discarded participants (see previous section) were not included since he deviated by more than one from the correct number of changes in one of the blocks (the rest of the participants did not exceed this deviation limit in any block).

Recording and pre-processing

Electroencephalographic (EEG) activity was recorded in the same electrically shielded room as in Experiment 1 also using an electrode active cap (Biosemi®) with the same 64 Ag-AgCl electrode array. Electrooculographic (EOG) data were recorded as in Experiment 1. Online and offline filters, sampling rate, epoch and baseline lengths, as well as the procedure to measure the lag between the triggers in EEG recordings and the actual stimulus onset on the screen were also identical.

As in Experiment 1, EEG epochs corresponding to trials in which the fixation dot changed its color to red, and the subsequent trial, were eliminated to avoid the effect of this control task. Blinking-derived artifact removal followed the same ICA-based strategy described in the previous experiment and also the automatic detection and deletion of trials procedure. In this case, the minimum number of trials accepted for averaging was 400 trials per participant and condition (i.e., spiders and wheels). Data from three of the discarded participants (see Participants section) were eliminated since they did not meet this criterion. Among those meeting it, the actual minimum of trials accepted for analysis was 410. This trial and participant rejection procedure led to the average admission of 451 (*SD=16*) in the case of spiders and of 452 (*SD=15*) in the case of wheels, the difference among stimulus categories being non-significant ($F(1,34)=0.137$, $p=0.714$, $\eta^2_p=0.004$).

Data availability

The data associated with this experiment are available at https://osf.io/9bc2y.

Data analysis

After baseline correction, the first analytic task was identifying and quantifying the first visual component of ERPs. As may be appreciated in Figure 4, a N40 component is clearly visible in grand averages, so the confirmation procedure carried out in Experiment 1 was not necessary this time. To define N40 peak latency, recordings at parietal and occipital electrodes, bilaterally, were averaged together to provide a meta-average (Figure 4). The latency of the most negative value of the meta-average between 30 and 60 ms was defined as the N40 peak, which was 45 ms. Therefore, N40 amplitude was individually quantified as the average amplitude within the 42 to 48 ms WOI. The next component in time (P100) was also quantified after defining its peak latency, which was defined from the same meta-average just mentioned (Figure 4). Thus, the latency of the most positive value within the meta-average between 70 and 130 ms was defined as the P100 peak, which was 105 ms. The WOI defined to quantify the average amplitude of this component was 99 to 111 ms. We also measured the differential N40-P100 amplitude, or peak to peak amplitude. To this aim, the individual difference between P100 and N40 amplitudes, each computed as explained above, was calculated (Figure 4).

*** Figure 4 ***

The same sPCA-based quantification method explained in Experiment 1 was again followed here on the WOIs corresponding to N40 and P100. Also, the double contrast strategy -frequentist and Bayesian- described in the previous experiment was again performed, using the same parameters, on factor scores yielded by sPCA introducing Emotion of the probe (spiders, wheels) as factor. Finally, the sources of N40 and P100 were estimated via the Minimum Norm (MN) source localization algorithm following the same specifications as in Experiment 1.

Results

The sPCA computed on N40 amplitudes yielded five SFs as explaining most of the variance of the 64 electrodes (89.87%). SF2 was the one showing similar distribution to the relevant N40-related spatial factor in Experiment 1. Neither frequentist ($t(34)= -0.403$, $p=0.345$, $d=-0.068$) nor Bayesian analyses ($BF_{10}=0.254$) indicated significantly greater amplitudes for spiders than for wheels. As for P100, five SFs explained 93.40% of the variance, with SF3 presenting similar distribution to that of the relevant P80 spatial factor in Experiment 1. Again, both frequentist ($t(34)= -0.925$, $p=0.819$, $d=-0.156$) and Bayesian contrasts ($BF_{10}=0.102$) failed to find significant spiders>wheels differences. Figures 4 and 5 show the topography of N40-SF2 and P100-SF3.

N40-P100 peak-to-peak amplitudes did show significant effects, as in Experiment 1. Six sPCA components were extracted (explaining 96.111% of the variance) and, among them, SF6 showed a midline-parietal distribution similar to the relevant N40-P80 factor in Experiment 1. The frequentist contrast revealed significantly greater N40-P100 peak-to-peak amplitudes for spiders than for wheels ($t(34)= 2.334$, $p=0.013$, $d=0.394$), and also did the Bayesian test ($BF_{10}=3.819$). Figure 5 depicts meta-averaged recordings from representative electrodes within SF6, along with descriptive plots. As in Experiment 1, and in order to test whether this significant sensitivity of N40-P100 peak-to-peak factor scores or amplitudes could be explained by either N40 or P100 alone, a repeated-measures ANCOVA was carried out following the same procedure: N40-P100 peak-to-peak amplitudes were introduced as dependent variable, and N40 and P100 amplitudes, separately, as covariates. The covariates were differently related to the N40-P100 peak-to-peak amplitude: while this relationship was significant in the case of N40 ($F(1, 44.581)=8.425$, $p=0.006$), it was not in the case of P100 ($F(1, 64.022)=1.386$, $p=0.243$). However, there was a significant effect of Emotion of the probe on N40-P100 peak to peak amplitude also after controlling for N40 and P100 individual amplitudes ($F(1, 30.596)=7.464$, $p=0.010$), suggesting additional mechanisms explaining this effect besides those reflected in these covariates.

*** Figure 5 ***

	Peak	WOI	SFs (% var)	T(34)	p	Cohen d's	BF_{10} (Bayes)
N40	45	42-48	5 (89.9)	-0.403	0.345	-0.068	0.254
P100	105	99-111	5 (93.4)	-0.925	0.819	0.516	0.102
N40-P100			6 (96.1)	**2.334**	**0.013**	**0.394**	**3.819**

Table 3. Experiment 2: peak latencies (in milliseconds), windows of interest (WOIs), number of spatial factors (SFs) extracted in sPCA, total variance they explain (% var), and outputs of both Student's frequentist and Bayesian t-tests on the spider>wheel difference corresponding to N40 and P100 amplitudes.

MN source estimation analysis on N40 was carried out on the average amplitude within the N40 and P100 WOIs, as indicated. As illustrated in Figure 4, this analysis yielded V1 as the net, main source (concretely, the caudal apex of the calcarine sulcus: x= -11, y= -105, z= -12). No other sources were observed in Experiment 2 for N40, probably due to the increased SNR provided by the methodological implementations previously mentioned. As for P100, the main source was located at V2/LOC (posterior part of the middle occipital gyrus: x= -45, y= -91, z= -3; see footnote 2). A second source for P100 was located in the superior parietal lobule (x= -26, y= -64, z=68).

N40		P100	
x, y, z	**Anatomical label**	**x, y, z**	**Anatomical label**
-11, -105, -12	Calcarine sulcus	-45, -91, -3	Middle occipital sulcus
		-26, -64, 68	Superior parietal lobule

Table 4. Experiment 2: Main sources estimated through the Minimum Norm method for N40 and P100 and their peak MNI coordinates.

Discussion

Experiment 2 revealed similar early visual ERP components as those found in Experiment 1. Thus, both an N40 (presenting slightly higher latency: 45 ms) and a subsequent positive component, P100 (peaking at 105 ms) were evident at parietal and occipital regions. The variations in latency of both components with respect to Experiment 1 are probably due, along

with the different sample of participants, to the implementations introduced in the experimental design. The most influential would be the variable ITI (instead of fixed), implemented to minimize alpha phase synchronization, which especially affects P1 latency (Gruber et al., 2005). Importantly, Experiment 2 also confirmed the emotional effect on peak-to-peak amplitude involving both components, N40-P100 in this case. Thus, this amplitude was significantly greater for spiders than for wheels also in Experiment 2. This replication reinforces the main finding in Experiment 1 and allows us to rule out that it was explained by possible confounding factors such as the contrast of the fixation dot over the background.

As in Experiment 1, this peak-to-peak amplitude effect was not explained by N40 or P100 separately, although the involvement of the former was stronger according to ANCOVAs. Moreover, neither N40 nor P100 showed significant effects when their single amplitude was analyzed. In this regard, Experiment 2 confirms the usefulness of analyzing peak-to-peak amplitudes in early visual ERPs, which appears to provide more complete and robust information (or less dependent on the experimental design) than single component analyses, at least when processes are transversal to two deflections rather than circumscribed to one of them, as seems to occur here. This classical way of measuring ERPs (e.g., Begleiter et al., 1980; Hillyard & Picton, 1978; Verleger & Cohen, 1978) has recently been revealed as useful to explore early visual ERP components (Carretié et al., 2022) and, as developed in the Data Analysis section of Experiment 1, is less affected by signal processing procedures such as filtering or baseline definition.

Increasing SNR in Experiment 2 also allowed us to obtain cleaner source estimations, particularly in the case of N40. This time, the origin of this component was clearly located in V1, with no other appreciable sources. The origin of P100 was also the visual cortex, although the contribution of V1 was not as evident as in the case of P80 (Experiment 1), probably due to its longer latency (≈25 ms). In line with previous studies, sources involved secondary areas

(Capilla et al., 2016; di Russo et al., 2012), concretely V2/LOC and the superior parietal lobule (SPL). The former source, involved in object recognition, was also observed and discussed in Experiment 1 with respect to P80, suggesting a -at least partial- functional link between P80 and P100. The SPL is a parietal area highly involved in attentional processes, both exogenous and endogenous, being a key node in the dorsal attention network (Corbetta et al., 2008). This parietal area is consistently involved in attentional capture by emotional distractors (i.e., irrelevant to the task, as in this case; Carretié, 2014). Moreover, this attentional capture by affective stimuli is typically reflected in P1, among other components (Carretié, 2014). Therefore, P100/P1 appears to reflect advanced stages of object identification (also observed in P80/C1, in Experiment 1), along with exogenous attention mechanisms.

GENERAL DISCUSSION

Previous studies place the earliest electrophysiological trace of emotional detection at around 80 ms from stimulus onset, concretely in the C1 component of ERPs (Acunzo et al., 2019; Carretié et al., 2022; Eldar et al., 2010; Pourtois et al., 2004). The two experiments confirm how quickly our visual system can detect certain emotional stimuli, but place this capability even earlier, starting at ≈40 ms from stimulus onset. This initial detection mechanism remains until ≈100 ms (P80 and P100 -which may be identified with traditional C1 and P1- in Experiments 1 and 2, respectively). The sources of this activity were located in visual cortices: V1 in the case of N40, both V1 and secondary cortices in the case of P80/C1, and mainly in secondary cortices in the case of P100/P1. This 40-100 ms window, reflected in the N40-C1P1 peak-to-peak amplitude, involves perceptual and attentional mechanisms, as indicated in previous discussions. Such mechanisms, implying interactions between those primary and secondary visual cortices, are transversal during the 40-100 window, rather than being circumscribed to a single ERP deflection.

This novel finding, and particularly its timing, has several important implications at the theoretical level as regards emotional processing, particularly with respect to the existing hypotheses on IESs. High-order structures such as the amygdala have been defended as a key IES capable of modulating the activity of the visual cortex, among other cerebral structures, at very short latencies (e.g., see reviews by Adolphs, 2008; Costafreda et al., 2008; Öhman, 2002; Zald, 2003). However, the latency of the amygdala's enhanced response to emotional stimuli is not compatible with present data. Concretely, and according to intracranial EEG recordings, the earliest amygdala response to non-facial emotional visual stimuli is beyond 150 ms (Méndez-Bértolo et al., 2016). Moreover, even the amygdalar response to facial expressions, which is faster as indicated in the Introduction, does not modulate visual cortex activity until more than 250 ms later (Wang et al., 2023). The alternatives to the amygdala hypothesis as an IES are currently under an open debate. On the one hand, the "central position" postulates that the sensory cortex itself "is responsible for smart (fast and precise) initial evaluation of environmental threat" (Li and Keil, 2023; p. 349). On the other hand, the "peripheral position" proposes that "beyond the central modulation of sensory experience, most sensory systems are tuned to conduct value-based appraisal of the environment before signals reach the cortex" (Kryklywy et al., 2020; p. 917).

The results of our two experiments point to non-amygdalar candidates to be IESs and, whereas they are compatible with both the central and the peripheral alternative hypotheses, this key issue is worth being -at least briefly- discussed. Emerging evidence points to the capability of earlier, first-order structures in the visual pathway such as the visual thalamus (see Carretié et al., 2021, for a review) or the superior colliculi (Méndez et al., 2022; non-human data) to modulate their activity depending on the salience of the stimulus without the concourse of the visual cortex. Even the activity of the retinal ganglion cells may be modulated by the emotional arousal level (Liang et al., 2020; non-human data). In our opinion, the key idea in this respect is that evaluation is a multistage process that requires all the steps (as each

depends on the previous one), both rudimentary and precise, both fast and slow, to be "smart" and to allow for adaptive coping with emotional situations. In this chain of evaluative stages, the visual cortex, the amygdala, and other evaluative structures, would play a crucial role in different moments. However, as for the *initial* stage, which is the scope of this study, the peripheral hypothesis seems better positioned according to the scarce data available so far. In any case, further research is needed to advance this debate.

A final remark on possible alternative interpretations should be made. While low-level visual parameters were controlled and homogenized between spiders and wheels, high-level differences apart from the emotional content exist between both categories. Particularly, these results could also be compatible with the possibility that the observed effects reflect fast non-emotional categorial processing (e.g., natural vs. artificial, or animals vs. objects). Although this possibility cannot be discarded, we consider it very remote. Thus, while emotional stimuli are, by definition, relevant for the individual, the natural or animal condition of an item is orthogonal to relevance. For example, and mentioning typical "animal/natural" items employed as emotional stimuli, relevance of a sparrow is minimal as compared to a snake for the majority of population (as revealed by normative data in emotional picture databases cited above); in the non-animal/artificial category, an empty pot vs. a pistol pointing at us would be a parallel example. Critically, the evolutionary pressure on an extremely swift evaluation mechanism would be higher to detect emotion/relevance than to carry out a semantic categorization. Moreover, semantic processing of stimulation occurs later in time according to current data (e.g., first traces of animal vs. non-animal discrimination occur beyond 100 ms: Cichy & Pantazis, 2017; Crouzet et al., 2012). In any case, this issue is worth being explored in the future by introducing additional stimulus categories and/or, in case fearful stimuli are employed, by manipulating individual fear, since high levels (or even phobia) would reinforce the observed effects in case emotional rather than semantic categorization explains them.

ACKNOWLEDGEMENTS

Funding: this work was supported by Ministerio de Ciencia e Innovación [MICINN; grant number PID2021-124420NB-I00).

REFERENCES

Acunzo DJ, MacKenzie G, van Rossum MCW. Systematic biases in early ERP and ERF components as a result of high-pass filtering. J Neurosci Methods. 2012;209:212-218.

Acunzo D, MacKenzie G, van Rossum MCW. Spatial attention affects the early processing of neutral versus fearful faces when they are task-irrelevant: A classifier study of the EEG C1 component. Cogn Affect Behav Neurosci. 2019;19:123-137.

Adolphs R. Fear, faces, and the human amygdala. Curr Opin Neurobiol. 2008;18:166-172.

Ales JM, Yates JL, Norcia AM. V1 is not uniquely identified by polarity reversals of responses to upper and lower visual field stimuli. Neuroimage. 2010;52:1401-1409.

Anzai A, Peng X, Van Essen DC. Neurons in monkey visual area V2 encode combinations of orientations. Nat Neurosci. 2007;10:1313-1321.

Azzopardi P, Cowey A. The overrepresentation of the fovea and adjacent retina in the striate cortex and dorsal lateral geniculate nucleus of the macaque monkey. Neuroscience. 1996;72:627-639.

Beck DM, Kastner S. Stimulus context modulates competition in human extrastriate cortex. Nat Neurosci. 2005;8:1110-1116.

Begleiter H, Porjesz B, Tenner M. Neuroradiological and neurophysiological evidence of brain deficits in chronic alcoholics. Acta Psychiatr Scand. 1980;62:3-13.

Bradley MM, Hamby S, Löw A, Lang PJ. Brain potentials in perception: picture complexity and emotional arousal. Psychophysiology. 2007;44:364-373.

Brown LE, Halpert BA, Goodale MA. Peripheral vision for perception and action. Exp Brain Res. 2005;165:97-106.

Buchner H, Gobbelé R, Wagner M, Fuchs M, Waberski TD, Beckmann R. Fast visual evoked potential input into human area V5. Neuroreport. 1997;8:2419-2422.

Capilla A, Melcón M, Kessel D, Calderón R, Pazo-Álvarez P, Carretié L. Retinotopic mapping of visual event-related potentials. Biol Psychol. 2016;118:114-125.

Carretié L. Exogenous (automatic) attention to emotional stimuli: A review. Cogn Affect Behav Neurosci. 2014;14:1228-1258.

Carretié L, Fernández-Folgueiras U, Álvarez F, Cipriani G, Tapia M, Kessel D. Fast unconscious processing of emotional stimuli in early stages of the visual cortex. Cereb Cortex. 2022;32:4331-4344.

Carretié L, Tapia M, López-Martín S, Albert J. EmoMadrid: An emotional pictures database for affect research. Motiv Emot. 2019;43:929-939.

Carretié L, Yadav RK, Méndez-Bértolo C. The missing link in early emotional processing. Emotion Rev. 2021;13:225-244.

Cichy RM, Pantazis D. Multivariate pattern analysis of MEG and EEG: A comparison of representational structure in time and space. Neuroimage. 2017;158:441-454.

Corbetta M, Patel G, Shulman GL. The reorienting system of the human brain: From environment to theory of mind. Neuron. 2008;58:306–324.

Costafreda SG, Brammer MJ, David AS, Fu CHY. Predictors of amygdala activation during the processing of emotional stimuli: A meta-analysis of 385 PET and fMRI studies. Brain Res Rev. 2008;58:57-70.

Crouzet SM, Joubert OR, Thorpe SJ, Fabre-Thorpe M. Animal detection precedes access to scene category. PLoS One. 2012;7(12):e51471.

Desimone R. Visual attention mediated by biased competition in extrastriate visual cortex. Philos Trans R Soc Lond B Biol Sci. 1998;353:1245-1255.

Di Russo F, Martínez A, Hillyard SA. Source analysis of event-related cortical activity during visuo-spatial attention. Cereb Cortex. 2003;13:486–499.

Di Russo F, Stella A, Spitoni G, Strappini F, Sdoia S, Galati G, et al. Spatiotemporal brain mapping of spatial attention effects on pattern-reversal ERPs. Hum Brain Mapp. 2012;33:1334–1351.

Dien J. Evaluating two-step PCA of ERP data with geomin, infomax, oblimin, promax, and varimax rotations. Psychophysiology. 2010;47:170-183.

Eldar S, Yankelevitch R, Lamy D, Bar-Haim Y. Enhanced neural reactivity and selective attention to threat in anxiety. Biol Psychol. 2010;85:252-257.

Faul F, Erdfelder E, Buchner A, Lang A. Statistical power analyses using G*Power 3.1: Tests for correlation and regression analyses. Behav Res Methods. 2009;41:1149-1160.

Ffytche DH, Guy CN, Zeki S. The parallel visual motion inputs into areas V1 and V5 of human cerebral cortex. Brain. 1995;118:1375-1394.

Fiebelkorn IC, Kastner S. Functional specialization in the attention network. Annu Rev Psychol. 2020;71:221-249.

Foxe JJ, Simpson GV. Flow of activation from V1 to frontal cortex in humans. Exp Brain Res. 2002;142:139-150.

Foxe JJ, Strugstad EC, Sehatpour P, Molholm S, Pasieka W, Schroeder CE, et al. Parvocellular and magnocellular contributions to the initial generators of the visual evoked potential: high-density electrical mapping of the “C1” component. Brain Topogr. 2008;21:11-21.

Gerdes AB, Uhl G, Alpers GW. Spiders are special: Fear and disgust evoked by pictures of arthropods. Evol Hum Behav. 2009;30:66-73.

Ghodrati M, Khaligh-Razavi S, Lehky SR. Towards building a more complex view of the lateral geniculate nucleus: Recent advances in understanding its role. Prog Neurobiol. 2017;156:214-255.

Gramfort A, Papadopoulo T, Olivi E, Clerc M. OpenMEEG: opensource software for quasistatic bioelectromagnetics. Biomed Eng Online. 2010;9:45.

Grill-Spector K, Kourtzi Z, Kanwisher N. The lateral occipital complex and its role in object recognition. Vision Res. 2001;41:1409-1422.

Gruber WR, Klimesch W, Sauseng P, Doppelmayr M. Alpha phase synchronization predicts P1 and N1 latency and amplitude size. Cereb Cortex. 2005;15:371-377.

Hillyard SA, Teder-Sälejärvi WA, Münte TF. Temporal dynamics of early perceptual processing. Curr Opin Neurobiol. 1998;8:202-210.

Hillyard SA, Picton TW. On and off components in the auditory evoked potential. Percept Psychophys. 1978;24:391-398.

Hubel DH, Wiesel TN. Laminar and columnar distribution of geniculo-cortical fibers in the macaque monkey. J Comp Neurol. 1972;146:421-450.

IBM Corp. IBM SPSS Statistics for Windows, Version 26. Armonk, NY: IBM Corp; 2019.

Inui K, Kakigi R. Temporal analysis of the flow from V1 to the extrastriate cortex in humans. J Neurophysiol. 2006;96:775-784.

Jacobi F, Wittchen HU, Hölting C, Höfler M, Pfister H, Müller N, et al. Prevalence, co-morbidity and correlates of mental disorders in the general population: results from the German Health Interview and Examination Survey (GHS). Psychol Med. 2004;34:597-611.

JASP Team. JASP (Version 0.15) [Computer software]. 2021.

Johannes S, Münte TF, Heinze HJ, Mangun GR. Luminance and spatial attention effects on early visual processing. Cogn Brain Res. 1995;2:189-205.

Jung TP, Makeig S, Humphries C, Lee TW, Mckeown MJ, Iragui V, et al. Removing electroencephalographic artifacts by blind source separation. Psychophysiology. 2000;37:163-178.

Kelly SP, Schroeder CE, Lalor EC. What does polarity inversion of extrastriate activity tell us about striate contributions to the early VEP? A comment on Ales et al. (2010). Neuroimage. 2013;76:442-445.

Ko HK, von der Heydt R. Figure-ground organization in the visual cortex: Does meaning matter? J Neurophysiol. 2018;119:160-176.

Kryklywy JH, Ehlers MR, Anderson AK, Todd RM. From architecture to evolution: multisensory evidence of decentralized emotion. Trends Cogn Sci. 2020;24:916-929.

Kybic J, Clerc M, Abboud T, Faugeras O, Keriven R, Papadopoulo T. A common formalism for the integral formulations of the forward EEG problem. IEEE Trans Med Imaging. 2005;24:12-28.

Lang PJ, Bradley MM, Cuthbert BN. International affective picture system (IAPS): Affective ratings of pictures and instruction manual. Gainesville, FL: University of Florida; 2005.

Liang L, Fratzl A, Reggiani JD, El Mansour O, Chen C, Andermann ML. Retinal inputs to the thalamus are selectively gated by arousal. Curr Biol. 2020;30:3923-3934.

Li W, Keil A. Sensing fear: fast and precise threat evaluation in human sensory cortex. Trends Cogn Sci. 2023;27:341-352.

Masri RA, Grünert U, Martin PR. Analysis of parvocellular and magnocellular visual pathways in human retina. J Neurosci. 2020;40:8132-8148.

Maunsell JH, Gibson JR. Visual response latencies in striate cortex of the macaque monkey. J Neurophysiol. 1992;68:1332-1344.

Méndez CA, Celeghin A, Diano M, Orsenigo D, Ocak B, Tamietto M. A deep neural network model of the primate superior colliculus for emotion recognition. Philos Trans R Soc B. 2022;377(1863):20210512.

Méndez-Bértolo C, Moratti S, Toledano R, Lopez-Sosa F, Martínez-Alvarez R, Mah YH, et al. A fast pathway for fear in human amygdala. Nat Neurosci. 2016;19:1041.

Mohr KS, Kelly SP. The spatiotemporal characteristics of the C1 component and its modulation by attention. Cogn Neurosci. 2018;9:71–74.

Moradi F, Liu LC, Cheng K, Waggoner RA, Tanaka K, Ioannides AA. Consistent and precise localization of brain activity in human primary visual cortex by MEG and fMRI. Neuroimage. 2003;18:595-609.

Nakashima T, Kaneko K, Goto Y, Abe T, Mitsudo T, Ogata K, et al. Early ERP components differentially extract facial features: evidence for spatial frequency-and-contrast detectors. Neurosci Res. 2008;62:225-235.

Öhman A. Automaticity and the amygdala: Nonconscious responses to emotional faces. Curr Dir Psychol Sci. 2002;11:62-66.

Oostenveld R, Fries P, Maris E, Schoffelen JM. FieldTrip: open source software for advanced analysis of MEG, EEG, and invasive electrophysiological data. Comput Intell Neurosci. 2011.

Paulus WM, Hömberg V, Cunningham K, Halliday AM, Rohde N. Colour and brightness components of foveal visual evoked potentials in man. Electroencephalogr Clin Neurophysiol. 1984;58:107-119.

Pourtois G, Grandjean D, Sander D, Vuilleumier P. Electrophysiological correlates of rapid spatial orienting towards fearful faces. Cereb Cortex. 2004;14:619-633.

Proverbio AM, Broido V, De Benedetto F, Zani A. Scalp-recorded N40 visual evoked potential: Sensory and attentional properties. Eur J Neurosci. 2021;54:6553– 6574.

Proverbio AM, Del Zotto M, Zani A. Electrical neuroimaging evidence that spatial frequency-based selective attention affects V1 activity as early as 40-60 ms in humans. BMC Neurosci. 2010;11:1-13.

Proverbio AM, Esposito P, Zani A. Early involvement of the temporal area in attentional selection of grating orientation: an ERP study. Cogn Brain Res. 2002;13:139-151.

Schroeder CE, Mehta AD, Givre SJ. A spatiotemporal profile of visual system activation revealed by current source density analysis in the awake macaque. Cereb Cortex. 1998;8:575-592.

Van Strien JW, Christiaans G, Franken IH, Huijding J. Curvilinear shapes and the snake detection hypothesis: an ERP study. Psychophysiology. 2016;53:252-257.

Verleger R, Cohen R. Effects of certainty, modality shift and guess outcome on evoked potentials and reaction times in chronic schizophrenics. Psychol Med. 1978;8:81-93.

Wang Y, Luo L, Chen G, Luan G, Wang X, Wang Q, et al. Rapid processing of invisible fearful faces in the human amygdala. J Neurosci. 2023;43:1405-1413.

Widmann A, Schröger E. Filter effects and filter artifacts in the analysis of electrophysiological data. Front Psychol. 2012;3:233.

Yoshida F, Hirata M, Onodera A, et al. Noninvasive spatiotemporal imaging of neural transmission in the subcortical visual pathway. Sci Rep. 2017;7:4424.

Zald DH. The human amygdala and the emotional evaluation of sensory stimuli. Brain Res Brain Res Rev. 2003;41:88-123.

Zhang W, Lu J. Time course of automatic emotion regulation during a facial Go/Nogo task. Biol Psychol. 2012;89:444-449.

Figure legends

Figure 1. A: Size and possible locations of the stimulus in each trial. **B:** Schematic representation of one portion of the stimulus sequence. One of the exemplars of spider and wheel probes are depicted, each in one of the five possible spatial locations.

Figure 2. Experiment 1: windows of interest (WOI) for N40 (blue bar), only found in FIX, and P80 (green bars), patent in all conditions. WOIs are represented over grand averages corresponding to each of the five locations where stimuli appeared (FIX: fixation, LL: lower left, LR: lower right, UL: upper left, UR: upper right). Temporal and amplitude scales are the same for all locations and are defined in FIX. Meta-averages are computed from the electrode sites marked in black in each scalp map. Topographic maps of sPCA-derived relevant factor scores corresponding to each WOI are also depicted, as well as source estimations corresponding to WOIs of FIX conditions, which were those finally showing significant effects (see Supplemental material for source estimations in the rest of conditions).

Figure 3. Experiment 1: descriptive data on N40, P80, and N40-P80 peak-to-peak factor scores (linearly related to amplitudes) in response to spiders and wheels presented at fixation in relevant spatial factors. Violin plots show individual distribution and line graphs show means and standard error of means (error bars). For illustrative purposes, grand averages (center) are computed from five representative electrodes (marked in red) within the regions of maximal factorial load.

Figure 4. Experiment 2: windows of interest (WOI) for N40 and P100 (green bars) WOIs are represented over grand averages Meta-averages are computed from the electrode sites marked in black in each scalp map. Topographic maps of the sPCA-derived relevant factor scores corresponding to each WOI are also depicted, as well as source estimations corresponding to WOIs.

Figure 5. Experiment 2: descriptive data on N40-P80 peak-to-peak factor scores (linearly related to amplitudes) in response to spiders and wheels in the relevant spatial factor. Violin plots show individual distribution and line graphs show means and standard error of means (error bars). For illustrative purposes, grand averages (center) are computed from three representative electrodes (marked in red) within the region of maximal factorial load.

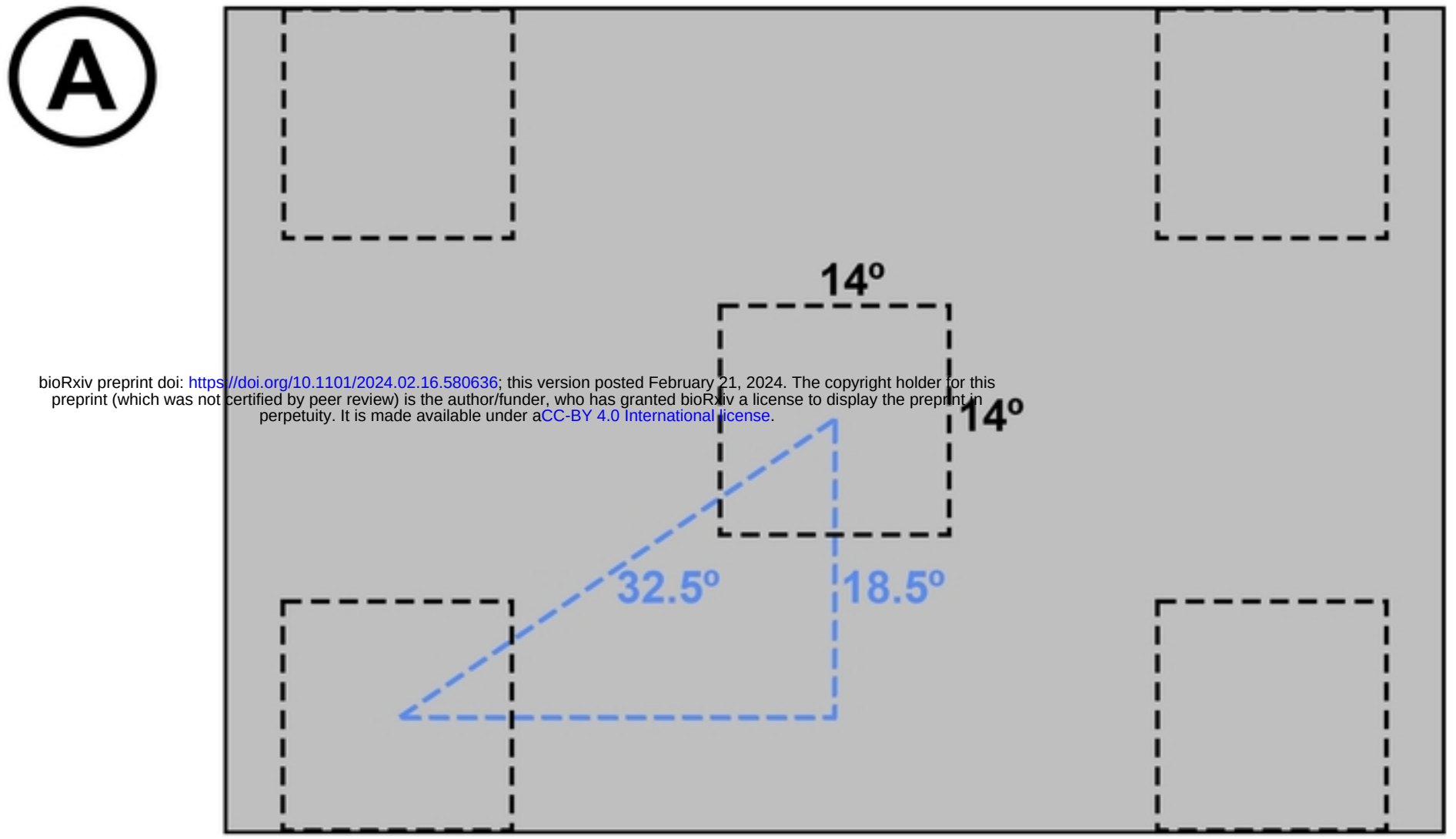

Figure 1

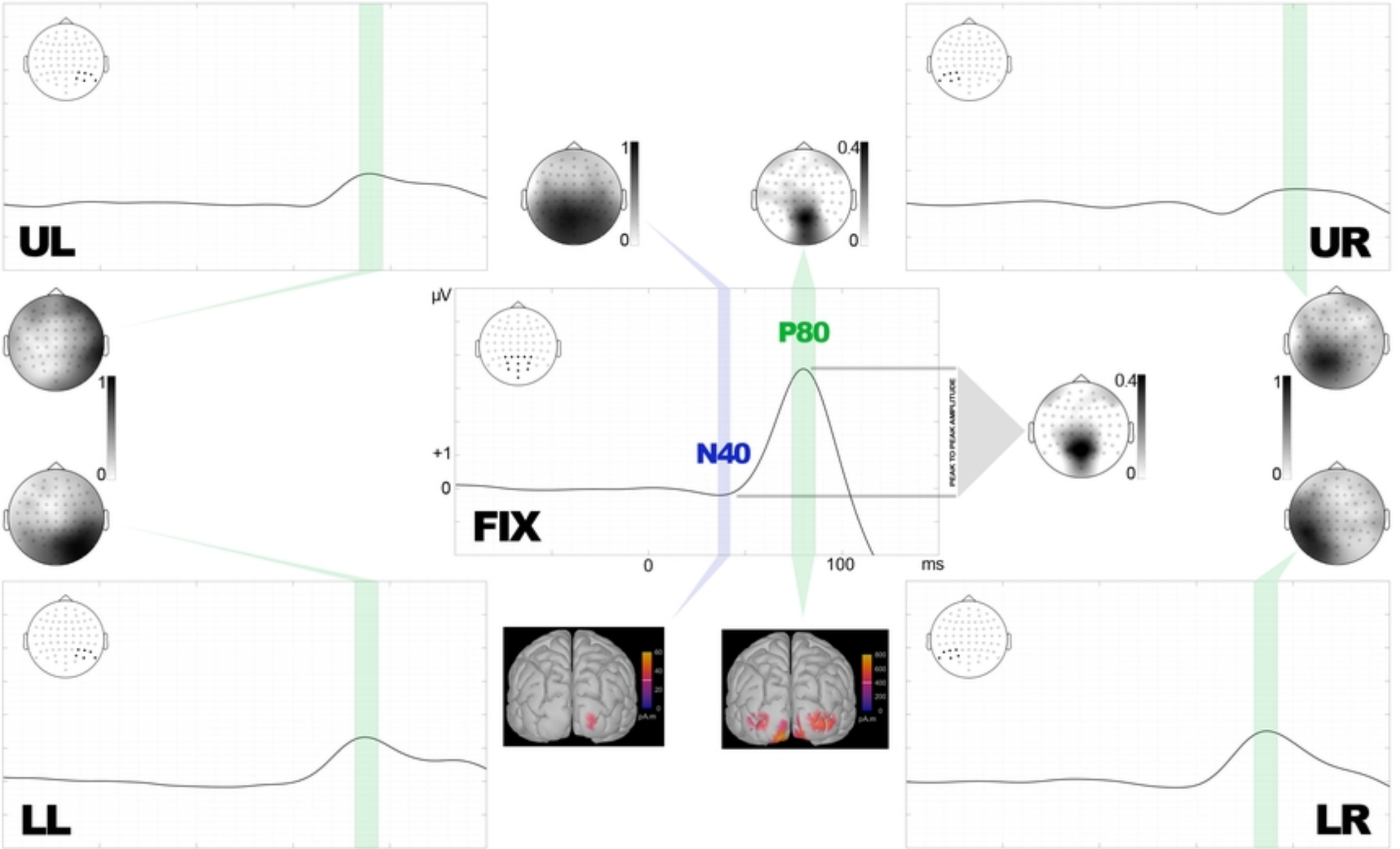
UL
UR
LL
LR
FIX
P80
N40
μV
+1
0
100
ms
PEAK TO PEAK AMPLITUDE
1
0
0.4
0

Figure 2

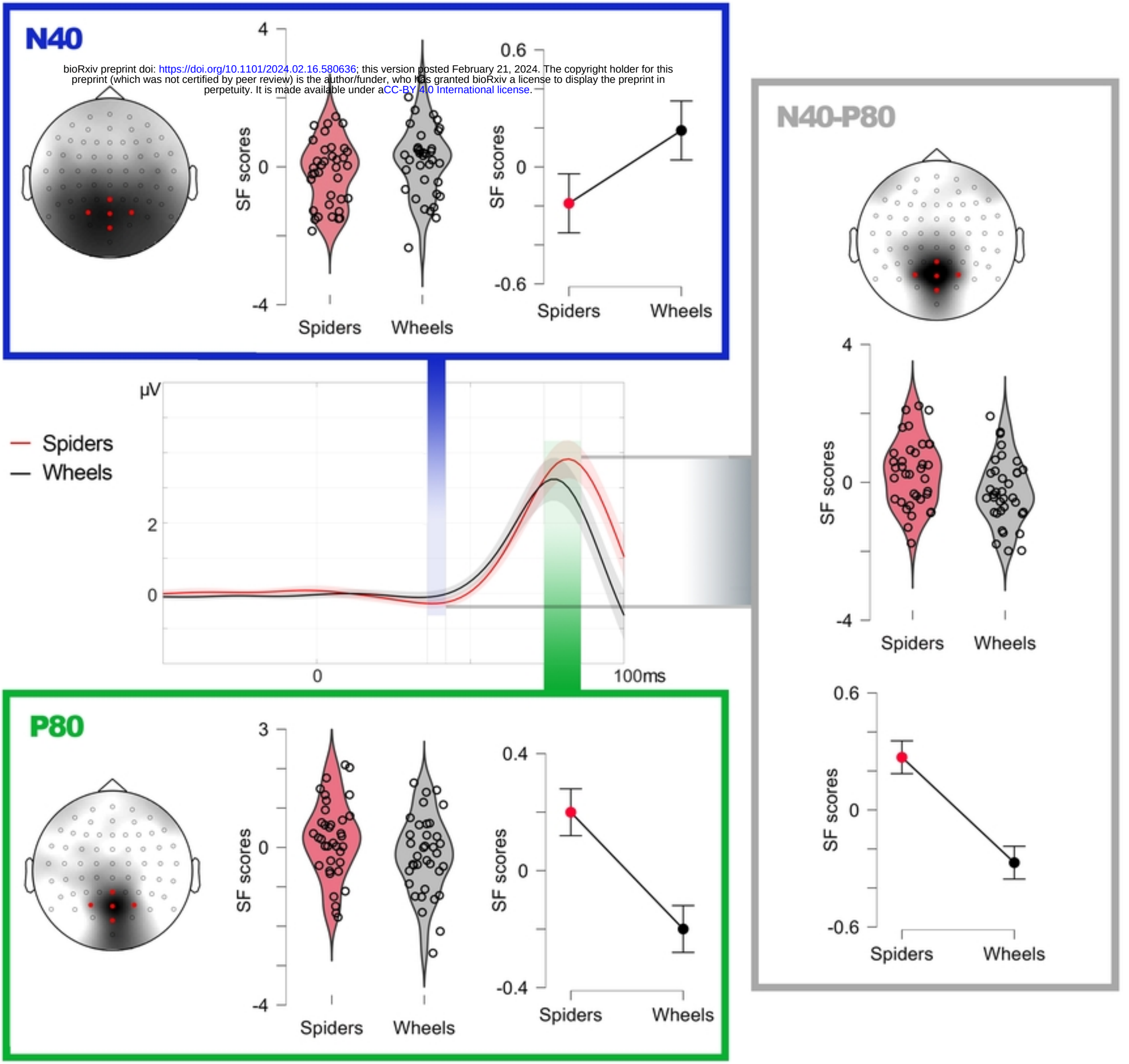

Figure 3

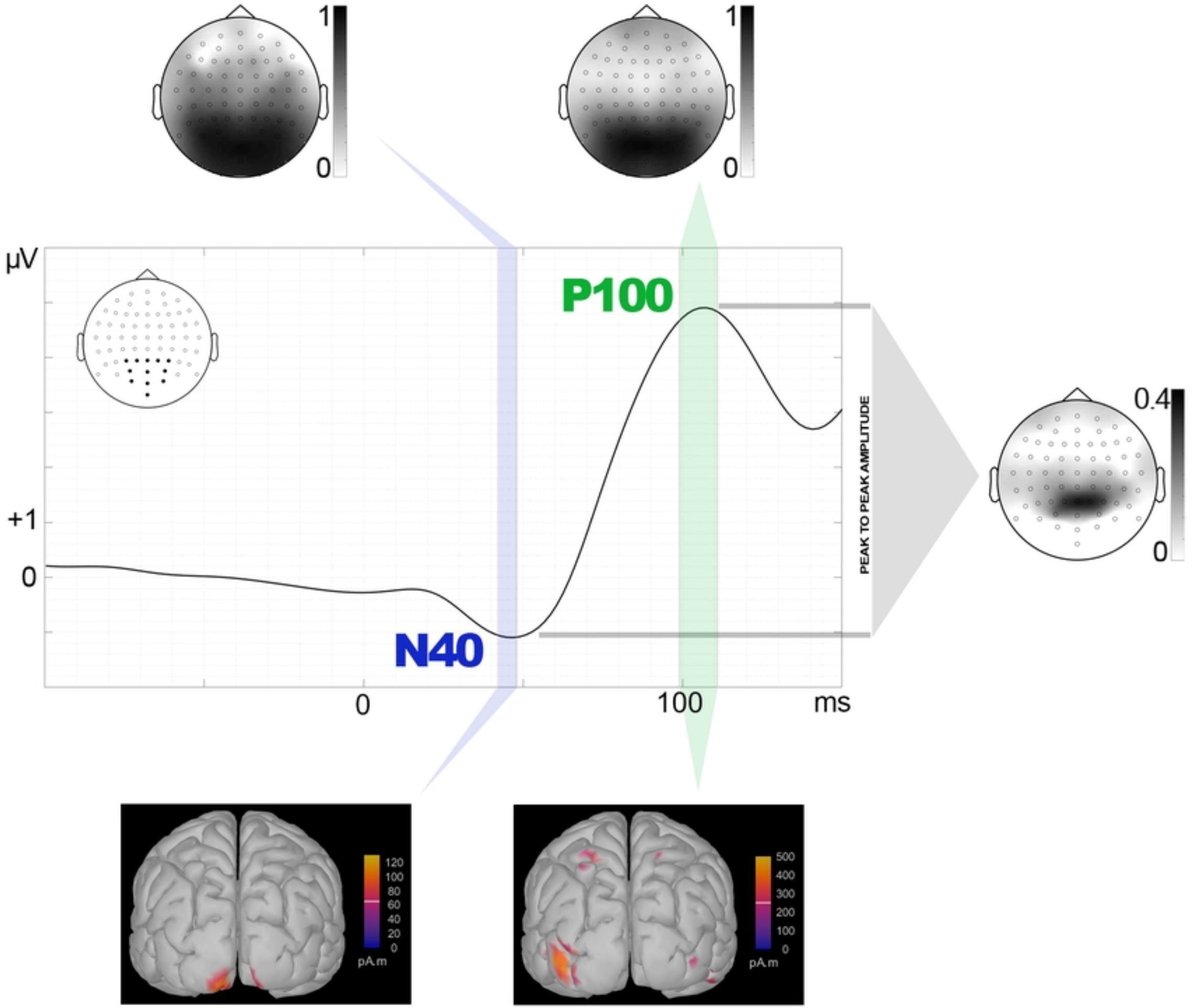
1
0
1
0
μV
+1
0
P100
N40
0
100
ms
PEAK TO PEAK AMPLITUDE
0.4
0
120
100
80
60
40
20
0
pA.m
500
400
300
200
100
0
pA.m

Figure 4

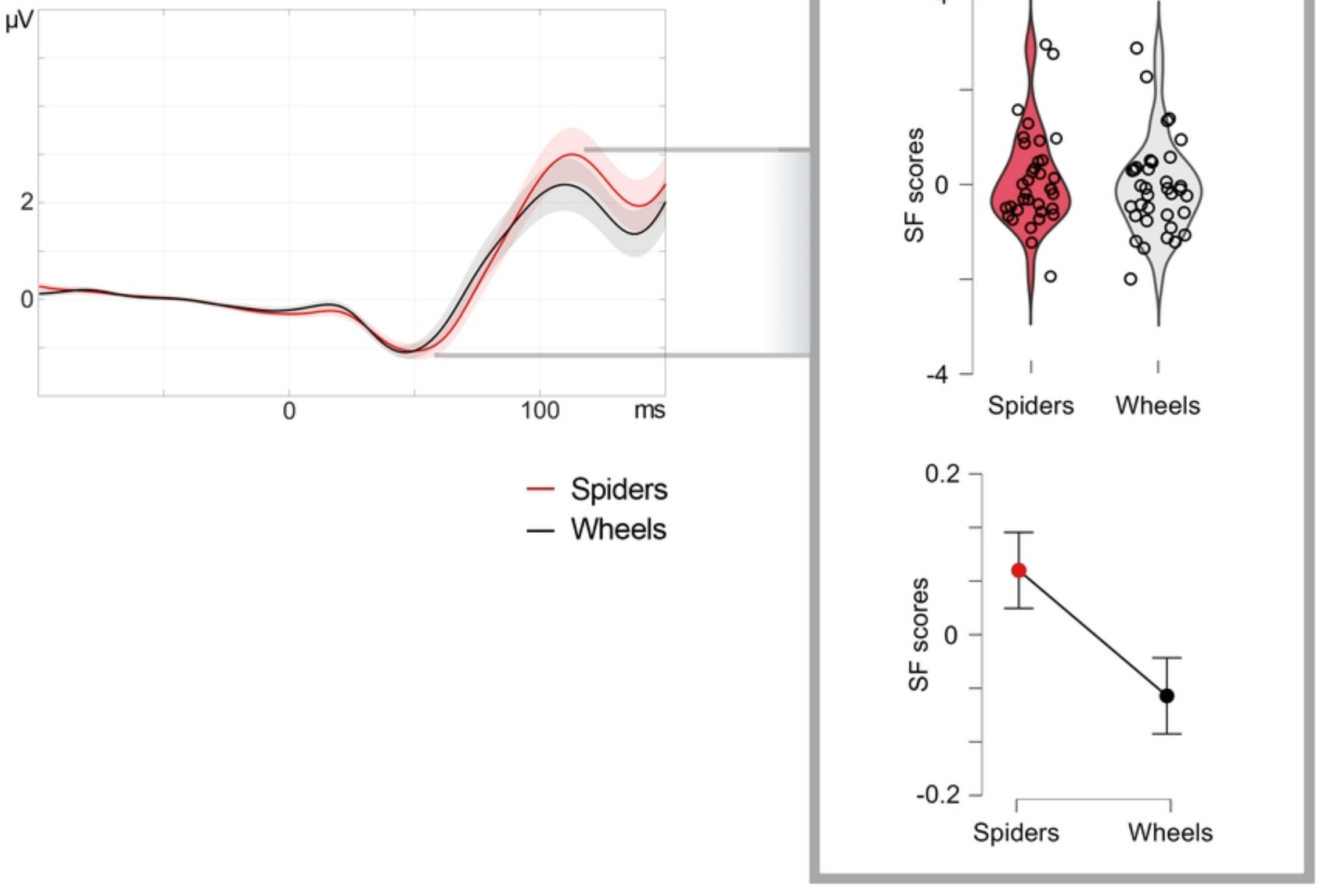

Figure 5